



ORIGINAL ARTICLE

Novel aromatic carboxamides from dehydroabietylamine as potential fungicides: Design, synthesis and antifungal evaluation



Zihui Yang, Qingsong Liu, Yue Sun, Xuebao Sun, Lu Sun, Linlin Chen, Wen Gu*

Jiangsu Provincial Key Lab for the Chemistry and Utilization of Agro-forest Biomass, Jiangsu Key Lab of Biomass-based Green Fuels and Chemicals, Co-Innovation Center for Efficient Processing and Utilization of Forest Products, College of Chemical Engineering, Nanjing Forestry University, Nanjing 210037, PR China

Received 23 May 2022; accepted 3 October 2022
Available online 9 October 2022

KEYWORDS

Dehydroabietylamine;
Aromatic derivatives;
Carboxamide;
Antifungal activity;
Succinate dehydrogenase inhibitor;
Molecular modeling

Abstract The present study was carried out to design and synthesize a number of novel aromatic carboxamide derivatives of dehydroabietylamine. The preliminary antifungal assay indicated that most of title compounds displayed moderate to good antifungal activity toward the six fungal strains *in vitro*. Compounds **3i**, **3q**, **4b** and **4d** showed significant antifungal activity against *Sclerotinia sclerotiorum*, with EC₅₀ values ranging from 0.067 ~ 0.393 mg/L. Compounds **3i**, **4b** and **4d** also showed pronounced mycelial growth inhibition activities against *B. cinerea* and *A. solani*. Furthermore, in the *in vivo* assay, compound **4b** exhibited brilliant protective activity against *S. sclerotiorum*-infected rape leaves. Meanwhile, the *in vivo* bioassay on tomato plants infected by *B. cinerea* showed that compound **3i** and **4d** displayed excellent protective activity at 200 mg/L, which were near to boscalid. Primary mechanistic study revealed that **4b** could inhibit sclerotia formation as well as reduce the exopolysaccharide level. SEM and TEM analysis indicated that **4b** possessed a strong ability to destroy the surface morphology of mycelia, cell structure and seriously interfere with the growth of the fungal pathogen. In addition, **4b** exhibited good inhibitory activity (IC₅₀ = 23.3 ± 1.6 μM) toward succinate dehydrogenase (SDH). Molecular modeling study confirmed the binding modes between compound **4b** and SDH. The above antifungal results and fungicidal mechanism study revealed that this class of dehydroabietylamine derivatives could be potential SDH inhibitors and lead compounds for novel fungicides development.

© 2022 The Author(s). Published by Elsevier B.V. on behalf of King Saud University. This is an open access article under the CC BY-NC-ND license (<http://creativecommons.org/licenses/by-nc-nd/4.0/>).

* Corresponding author.

E-mail address: njguwen@163.com (W. Gu).

Peer review under responsibility of King Saud University.



1. Introduction

Fungicides, which are one of the most important types of pesticides, could control plant diseases caused by various plant pathogenic fungi. In fact, the application of fungicides has become one of the most economical and effective ways to reduce the huge loss caused by fungal pathogens in agriculture (Fisher et al., 2012; Pennisi, 2010; Brown, 2002). However, the widespread application and misuse of fungicides caused huge threat to the fragile ecosystem and human's health. Moreover, the increasing resistances of fungal pathogens have emerged to be the main problem that would enhance the risk to global food safety (Liu et al., 2016; Yoon et al., 2013; Mitani et al., 2001; Wang et al., 2013). Thereby to discover more effective and environmental-friendly antifungal agrochemicals has strikingly drawn researcher's concern.

SDH has been recognized as the key component of respiratory enzyme complexes in the pivotal biochemical process. Its physiological function is to catalyze succinate oxidation coupling with electron transfers from succinate to ubiquinone (Yao et al., 2017a, 2017b; Sun et al., 2005; Jin et al., 2017; Liang et al., 2021; Yang et al., 2019). Over the past sixty years, continuing studies have confirmed that inhibiting the normal physiological function of SDH within phytopathogenic fungi could be an effective strategy to control the fungal infections in grains, vegetables and fruits, and the SDH enzyme was also the key target site for novel fungicide design (Yan et al., 2019; Liu et al., 2020; Liu et al., 2020). To date, twenty-four fungicides based on SDHs have been commercialized. However, the unlimited use of such fungicides also led to the resistance of pathogenic fungi. Therefore, there are still urgent needs for novel structures of SDHs to ensure the high yield and quality of crop production.

Natural products have been regarded as a rich and promising source for the candidates in the discovery of novel small molecule pesticides. Among them, some naturally occurring abietane-type diterpenoids and semisynthetic derivatives have displayed notable antifungal activity. For example, several abietane type diterpenoids isolated from *Taxodium distichum* Rich. were evaluated for antifungal activity against two wood rot fungi *Trametes versicolor* and *Fomitopsis palustris*. Two diterpenoids taxodione and 14-deoxycoleon U showed significant antifungal activities against two fungal strains (Kusumoto et al., 2010). Ferruginol, an abietane diterpene carnosic acid found in Labiatae herb, sage and rosemary, has profound antifungal activity against wood rot fungi. Mechanism study indicated that ferruginol could cause cell dysfunction of *T. versicolor* including microtubule disruption, reduction in self-defensive capability, inhibition of DNA repair and up-regulation of autophagy-related protein (Chen et al., 2015). Recently, some 1,3,4-thiadiazole-thiazolidinone derivatives of dehydroabietic acid were reported to show significant antifungal activity toward *Gibberella zeae* (Chen et al., 2016). Dehydroabietylamine (DHAAM), as an abietane-type diterpenoid derivative, was an important modified product of dehydroabietic acid obtained from *Pinus rosin* (Cai et al., 2022). Some synthetic derivatives of DHAAM exhibited significant and diverse biological activities such as antibacterial, antioxidant, antiviral, antileishmanial, antimalarial and anticancer activities (Salehi et al., 2014; Roa-Linares et al., 2016; Dea-Ayuela et al., 2016; Sadashiva et al., 2015; Liu et al., 2013). Meanwhile, only a few literatures have reported the synthesis of DHAAM derivatives exhibiting pronounced antifungal activity to plant pathogenic fungi. Tao et al. has synthesized dehydroabietyl-based amide derivatives with thiophene group, and some derivatives displayed significant antifungal activity toward *B. cinerea* *in vitro* and *in vivo*, which was stronger than the positive control penthiopyrad (Tao et al., 2020). Mao et al. designed and synthesized rosin-based 1,3,4-thiadiazole derivatives (Mao et al., 2021). The *in vivo* antifungal results demonstrated excellent protective effect on cucumber plants. Gao et al. has synthesized rosin-based acyl-thiourea compounds, which displayed moderate *in vitro* antifungal activity against *T. cucumeris* (Gao et al., 2018).

Heterocyclic compounds have received extensive attentions in the research of fungicides due to their noticeable antifungal activities (Zhang et al., 2018a, 2018b; Zhang et al., 2019). Specifically, pyridine, furan, thiazole and pyrazole rings were all important pharmacophores frequently used in SDHI fungicide design (Yao et al., 2017a, 2017b; Wu et al., 2021; Yu et al., 2020). For example, thifluzamide, which was invented by Dow Agrosience, showed excellent antifungal activity against *Rhizoctonia solani* causing sheath blight in rice paddy (Guo et al., 2019). Boscalid, fenfuram and bixafen with pyridine, furan, and pyrazole heterocycles, respectively, displayed excellent antifungal activities against a variety of plant pathogenic fungi (Fishel and Dewdney, 2015; Syngenta, 2020). Moreover, most reported SDH inhibitors contain the common carboxamide moiety as the key active group (Liu et al., 2019). Therefore, incorporating different types of heterocycles into the scaffold of DHAAM through the carboxamide linker may probably produce novel dehydroabietyl-based antifungal derivatives (Fig. 1). According to this assumption, a series of novel dehydroabietylamine derivatives containing carboxamide group were designed and synthesized. The antifungal potentials against six plant pathogenic fungi were also evaluated. Moreover, the *in vivo* antifungal assays on rape leaves and tomato plants was conducted to further evaluate the antifungal activity of some active compounds. SEM and TEM analysis were performed to observe the morphological features of fungal pathogens. Mechanism studies such as SDH enzyme inhibition activity and molecular dynamics simulation of the active compounds were also presented in this work.

2. Materials and methods

2.1. General

All reagents and solvents were analytical grade. Thin-layer chromatography (TLC) and column chromatography was conducted on silica gel (200 ~ 300 mesh), which were both purchased from Qingdao Marine Chemical Factory, China. ¹H NMR and ¹³C NMR spectra were generated from Bruker AV-400 and AV-600 spectrometers (Bruker Co. Ltd, Switzerland). Other instruments were utilized similar with our previous report. (Yang et al., 2021).

2.2. Synthetic procedure

The synthesis methods of intermediate **1** and dehydroabietylamide (**2**) were referenced by previously reported method (Gao et al., 2018; Nian et al., 2018). The reaction mixture of aromatic acid (1.20 mmol) and dehydroabietylamine (**2**, 1.0 mmol) were dissolved in 10 mL of CH₂Cl₂. 1-Ethyl-3-(3-dimethylpropylamine)carbodiimide (EDCI, 1.20 mmol) and 4-dimethylaminopyridine (DMAP, 0.10 mmol) were added into the solution. The mixture was stirred at 25 °C and monitored by TLC. When the reaction completed, the organic phase was washed with water (3 × 10 mL) and brine (3 × 10 mL), dried and concentrated *in vacuo*. The crude products were further purified by Silica gel column chromatography to give the title compounds **3a-3z**, **4a-4f** and **5a-5e**. The data and spectra of title compounds could be seen in [supporting information](#).

2.3. Antifungal activity of title compounds *in vitro*

Six plant pathogenic fungal strains, *Rhizoctonia solani* (*R. solani*), *Fusarium oxysporum* (*F. oxysporum*), *Sclerotinia sclerotiorum* (*S. sclerotiorum*), *Botrytis cinerea* (*B. cinerea*), *Ascochyta blight* (*A. blight*) and *Alternaria solana* (*A. solana*) were used for antifungal activity evaluation.

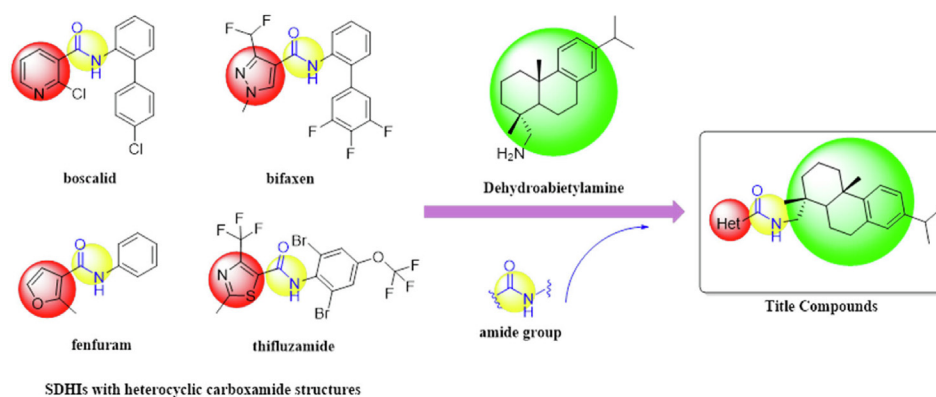


Fig. 1 Design strategy of the title compounds.

rotiorum (*S. sclerotiorum*), *Alternaria solani* (*A. solani*), *Gibberella zeae* (*G. zeae*) and *Botrytis cinerea* (*B. cinerea*) were obtained by Agricultural Culture Collection of China (ACCC). The antifungal activities of all newly synthesized carboxamide derivatives **3a-3z**, **4a-4f** and **5a-5e** were evaluated *in vitro* against above crop pathogenic fungi by the mycelium growth rate method based on the previous report. (Zhang et al., 2018a, 2018b). The stock solutions of the title compounds were prepared by dissolving each compound in DMSO at a concentration of 10 g/L. Then the stock solution was added and mixed to potato dextrose agar (PDA) medium to obtain the primary concentration (50 mg/L). Boscalid was assayed as a positive control and DMSO mixed with PDA was used as the blank control. The mycelial disks (5.0 mm) of each phytopathogenic fungus were inoculated on PDA plates at 25 °C. After an incubation period (3–7 days), the diameters (mm) of inhibition zones were measured by the cross-bracketing method. Each compound was measured in triplicate, and EC₅₀ values of active compounds were calculated with the concentration-dependent curves by using SPSS v.22.0 software.

2.4. *In vivo* bioassay on rape leaves infected by *S. Sclerotiorum*

The detailed experimental procedures of *in vivo* bioassay of compound **4b** were performed by previously reported methods (Yang et al., 2021). The susceptible rape leaves were collected from planting base of Nanjing Forest University. Healthy rape leaves were sprayed with compounds **4b** and boscalid (positive control) at the dosages of 100 or 200 mg/L, and subsequently cultivated for 24 h before inoculation with *S. sclerotiorum* respectively. Results were observed as diameters of symptoms after cultivation for 5 days at 25 °C. There were nine replicates for each treatment. The protective activity rate (%) was calculated as the following formula: (diameter of lesion in negative control – diameter of lesion in the treatment)/diameter of lesion in the negative control.

2.5. *In vivo* bioassay on tomato plants infected by *B. Cinerea*

The tomato plants were purchased from Suojincun Agricultural Market in Nanjing City. The detailed experimental procedures of *in vivo* testing were performed by previously reported methods (Wang et al., 2017). The tomato plants were

also used to evaluate *in vivo* antifungal activity. Conidia of *B. cinerea* obtained from 4-week-old cultures on PDA plates were suspended in 0.5 % (v/v) Tween-80 solution to ensure 1×10^6 spores per mL. When tomato plants grew to about 30 leaves, the solutions of the tested compounds (**3i**, **4b** and **4d**) and positive controls (boscalid) at the concentration of 200 mg/L were sprayed evenly onto tomato leaves. After dried naturally, these tomato plants were sprayed with prepared spore suspension, the tomato plants were maintained at 24 ± 1 °C and above 80 % relative humidity in greenhouse. The disease index was investigated when the untreated tomato plants developed symptoms, and then the control efficacy was calculated.

2.6. *Sclerotia* formation inhibition assay

The mycelial disks of *S. sclerotiorum* were inoculated on PDA mediums containing three concentrations (0.2, 0.1 and 0.05 mg/L) of **4b** and boscalid. The PDA mediums were cultured at 25 °C in the dark for 2 weeks. All sclerotia were collected and dried at 60 °C for 1 day. Then the weight of sclerotia and sclerotia formation inhibition were calculated.

2.7. Effect of compound **4b** on exopolysaccharide of *S. Sclerotiorum* strains

S. sclerotiorum strain was cultured in PDB medium for logarithmic growth phase, and then the fungal suspension was added into 25 mL PDB medium with compound **4b** at dosages of 0.2, 0.1 and 0.05 mg/L, which was incubated for 3 days in a rotary shaker (180 rpm, 28 °C). Then the precipitated mycelium was removed by centrifugation (12000 rpm, 4 °C for 30 min), and 75 mL ethanol was added into the liquidator for precipitation overnight. Further, the precipitation was collected by centrifugation (12000 rpm, 4 °C for 30 min) to get extracellular polysaccharide (EPS) crude product. Then all the treated samples were dried to constant weight at 70 °C. Each treatment was tested for three replicates. The mass of exopolysaccharide for each treatment was measured.

2.8. SEM observations

SEM observations were carried out to study the effects of **4b** on *S. sclerotiorum* microstructure. After treating with DMSO

(control), compound **4b** (3.125 mg/L, 0.781 mg/L and 0.195 mg/L) and positive control boscalid (3.125 mg/L, 0.781 mg/L and 0.195 mg/L) for 72 h, mycelia blocks (5.0 mm × 4.0 mm) were sheared from PDA plates. All the samples were treated by 4 % glutaraldehyde for 4 h. Each sample was then dehydrated with graded ethanol series (20, 50, 80, and 90 %) for 10 min. Then, all samples were dried, observed and photographed by using scanning electron microscope with 20 μm resolution ratio (Wang et al., 2021).

2.9. TEM observations

After treatment with compound **4b** (0.067 mg/L) for three days, the mycelial blocks of *S. sclerotiorum* on PDA plates were harvested, dehydrated and embedded in resin at 70 °C for 1 day, and then cut into thin sections. After the samples were double-stained with uranyl acetate and lead citrate, the morphology and ultrastructure of hyphae cells were observed by a transmission electron microscope (JEM-1400, JEOL, Ltd., Tokyo, Japan).

2.10. Cell cytotoxicity

The cytotoxicity of compounds **4b**, **4d** and boscalid in A549 cells (human lung adenocarcinoma cell line) were determined by following the MTT assay methods (Fei et al., 2021). The results were expressed in terms of cell viability and IC₅₀ for each compound.

2.11. In vitro SDH inhibition assay

The procedure of SDH inhibition assay *in vitro* was carried out by consulting some previous reports (Cheng et al., 2021; Lu et al., 2021; Zhang et al., 2019).

2.12. Molecular modeling

2.12.1. Homology modelling

The NCBI protein database (<https://www.ncbi.nlm.nih.gov/protein>) was used to search the SDH amino acid sequence of *S. sclerotiorum*. The employed hypothetical protein sequences were XP_001591238, XP_001594577, XP_001597467, and XP_001593251, reported by Birren. We applied succinate dehydrogenase from porcine heart (PDB ID: 1ZOY) as the template, and the three-dimensional (3D) structure of the SDH was obtained by SWISS-MODEL, a fully automated protein structure homology-modelling server (<https://swiss-model.expasy.org/>).

Molecular docking study was performed to investigate the binding mode between the compound and the *S. sclerotiorum* SDH using Autodock vina 1.1.2 (Trott and Olson, 2010). The 3D structure of the compound was built by ChemBio-Draw Ultra 14.0 and ChemBio3D Ultra 14.0 softwares. The AutoDockTools 1.5.6 package (Sanner, 1999; Morris et al., 2009) was employed to generate the docking input PDBQT files. The gridbox of the SDH was set as center_x: 86.459, center_y: 65.6, and center_z: 85.537 with dimensions size_x: 15, size_y: 15, and size_z: 15. The value of exhaustiveness was set to 20. The default parameters were used if it was not men-

tioned. Then an MD study was performed to revise the docking result.

2.12.2. Molecular dynamics simulation

The Amber 14 (Pierce et al., 2012; Götz et al., 2012; Salomon-Ferrer et al., 2013) and AmberTools 15 programs were used for MD simulations of the selected docked pose. The ligand was first prepared by ACPYPE (Da Silva and Vranken, 2012), a tool based on ANTECHAMBER (Wang et al., 2004; Wang et al., 2006) for generating automatic topologies and parameters in different formats for different molecular mechanics programs. Subsequently, the produced file was introduced to tleap program where Amber-ff14SB force fields implemented in AmberTools 15 were recruited to generate Amber topology and initial coordinates files. The solvated complex was submitted to a short energy minimization process including 2500 steps of steepest descent and 2500 steps of conjugate gradient followed by a 1000 ps heating step from 0 K to 300 K, and 500 ps of density equilibration with weak restraints using the GPU accelerated PMEMD (Particle Mesh Ewald Molecular Dynamics) module. The final production of dynamic simulation was performed for 30 ns under periodic boundary condition where no constraint was applied to the protein.

Binding energies (ΔG_{bind} in kcal/mol) were calculated for ligand-receptor complexes using the Molecular Mechanics/Generalized Born Surface Area (MM/GBSA) method. Moreover, to identify the key protein residues responsible for the ligands binding process, the binding free energy was decomposed on a per-residue basis. All the molecular dynamics were performed on a Linux-based (Ubuntu 14.04) GPU workstation.

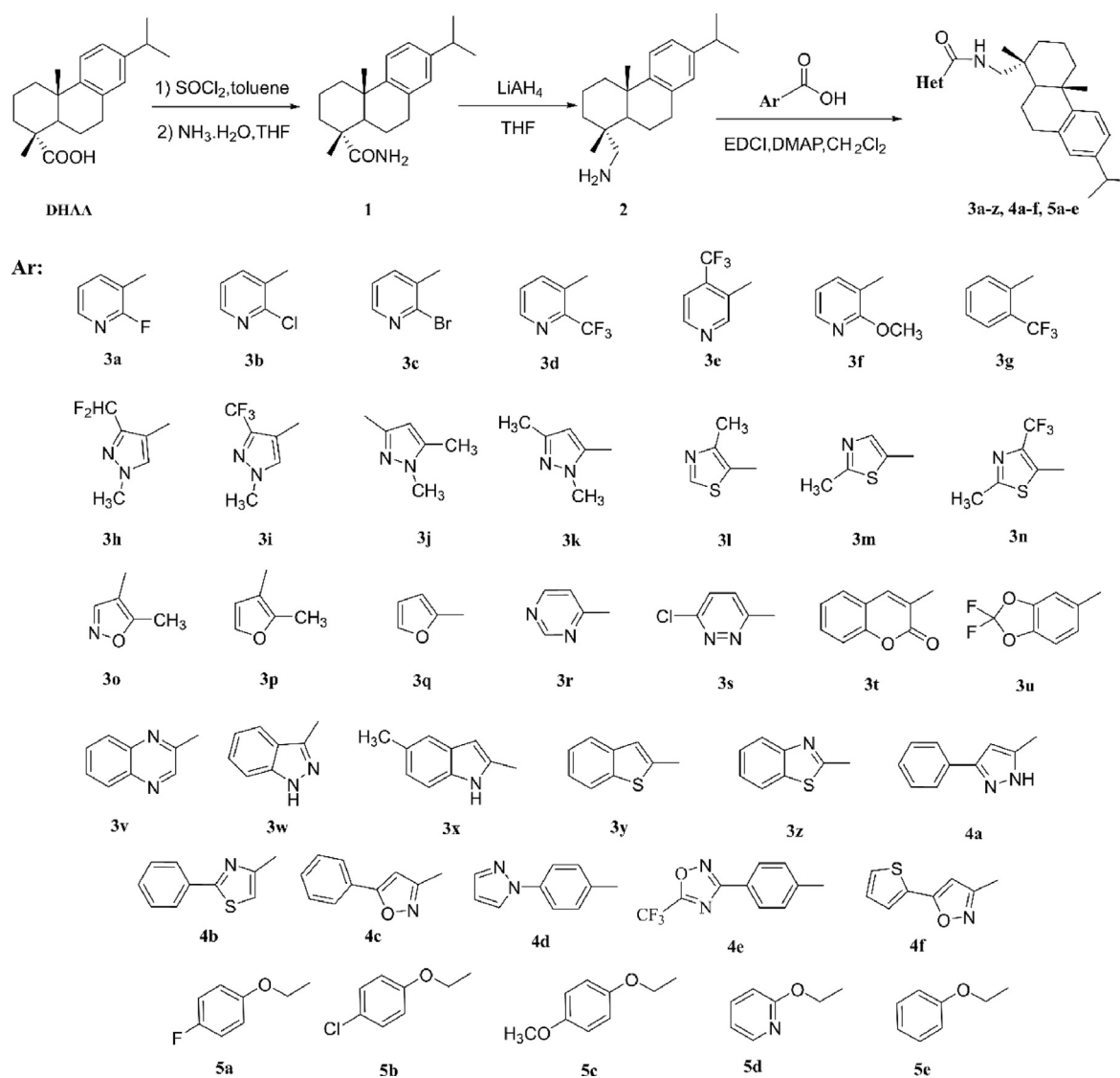
3. Results and discussion

3.1. Chemistry

The synthetic route for title compounds was shown in Scheme 1. Dehydroabiatic acid (DHAA) was used as the starting materials, and key intermediate dehydroabietylamine (**2**) was synthesized *via* two step (amide reaction and reduction reaction). Then, intermediate **2** was reacted with different aromatic acid to give title compounds **3a-3z**, **4a-4f** and **5a-5e** *via* amide reaction under mild condition. The structures were confirmed by their NMR and HRMS spectroscopic data.

3.2. In vitro antifungal activity

Comparing with the commercial fungicide boscalid, all compounds were screened for their *in vitro* antifungal activity toward six plant pathogenic fungi at 50 mg/L. *In vitro* antifungal activities of compounds **3a-3z**, **4a-4f** and **5a-5e** were listed in Table 1, which displayed the mycelial growth inhibitory rates of compounds **3a-3z** against six representative fungi at 50 mg/L. Some compounds effectively inhibited the *in vitro* mycelium growth of *S. sclerotiorum*. Several of them demonstrated fair to excellent mycelial growth inhibition activities against *S. sclerotiorum*, *A. solani* and *B. cinerea*. Notably, compound **3i** and **3q** exhibited more than 95 % inhibitory rates



Scheme 1 Synthetic route for the title compounds **3a-3z**, **4a-4f** and **5a-5e**.

toward *S. sclerotiorum*, which were approached with boscalid (100 %). Compounds **3e**, **3o**, **3l** and **3m** also showed considerable anti-*S. sclerotiorum* effects with inhibition rates ranging from 80 % to 95 %. For *A. solani*, compounds **3i** and **3o** showed the same level inhibitions with boscalid (91.8 %). For *B. cinerea*, only compound **3i** displayed more than 90 % inhibitory rate, which was superior over boscalid (75.3 %). For *G. zeae*, five compounds (**3e**, **3i**, **3l**, **3o**, **3s**) presented more than 80 % inhibitory rate. Overall, a majority of compounds **3a-3z** showed mild or poor mycelial growth inhibition activities against *R. solani* and *F. oxysporum* with 0 ~ 70 % inhibition, except that compounds **3i** and **3q**, which exhibited more than 70 % inhibition rates against *R. solani*. On the whole, compounds **3i** and **3q** showed broad-spectrum antifungal activities to all test strains.

Among compounds **4a-4f** and **5a-5e** (Table 1), some of them exhibited good mycelial growth inhibitory activities toward *A. solani* and *S. sclerotiorum*. On the other hand, most of them demonstrated moderate activities against *B. cinerea*

and *G. zeae*. However, a majority of them displayed inferior inhibition against *F. oxysporum* and *R. solani* than boscalid, which were similar with compounds **3a-3z**. In detail, two compounds (**4b** and **4d**) exhibited impressive anti-*S. sclerotiorum* effects with the corresponding inhibition rates of 98.4 % and 99.2 %, which approached to boscalid (100 %). Besides, **4e** and **5a** showed good antifungal activity against *S. sclerotiorum*. For *B. cinerea*, compound **4b** and **4d** also exhibited excellent antifungal activity, which were significantly better than boscalid.

To assess the fungicidal potency, the EC₅₀ values of active compounds with inhibitions over greater than 98 % against *S. sclerotiorum* were examined. The results in Table 2 suggested that compounds **3i**, **3q**, **4b** and **4d** obviously inhibited *S. sclerotiorum* with EC₅₀ values of 0.067 ~ 0.393 mg/L. Remarkably, compound **4b** exhibited the promising antifungal activity (EC₅₀ = 0.067 mg/L), which were superior over boscalid (EC₅₀ = 0.118 mg/L). **4d** also displayed good mycelial growth inhibition (EC₅₀ = 0.092 mg/L), which was compara-

Table 1 *In vitro* antifungal activities of DHAA, **2**, and compounds **3a–3z**, **4a–4f** and **5a–5e** at 50 mg/L.

Compd	Inhibition rate (%) ^a					
	<i>R. solani</i>	<i>B. cinerea</i>	<i>F. oxysporum</i>	<i>S. sclerotiorum</i>	<i>A. solani</i>	<i>G. zeae</i>
DHAA	40.8 ± 1.0	53.9 ± 2.2	42.0 ± 1.0	52.9 ± 0.8	56.9 ± 1.2	39.0 ± 1.8
2	32.5 ± 1.0	46.6 ± 0.8	23.6 ± 2.0	32.9 ± 0.8	72.2 ± 1.2	51.9 ± 1.6
3a	15.3 ± 1.1	20.0 ± 0.1	28.5 ± 1.7	4.78 ± 1.7	11.1 ± 5.5	21.3 ± 0.8
3b	26.2 ± 1.3	16.9 ± 0.1	20.3 ± 2.8	21.5 ± 1.2	64.3 ± 0.1	27.9 ± 8.0
3c	29.0 ± 5.3	0	13.6 ± 0.1	28.2 ± 2.9	20.6 ± 3.6	42.3 ± 1.8
3d	26.5 ± 2.2	19.0 ± 3.6	31.2 ± 3.6	40.4 ± 3.3	7.9 ± 2.7	31.4 ± 0.4
3e	61.7 ± 1.0	24.1 ± 1.8	1.7 ± 1.5	91.6 ± 0.6	69.8 ± 1.4	83.2 ± 1.2
3f	6.5 ± 0.1	9.7 ± 3.5	17.3 ± 0.1	17.0 ± 4.5	52.3 ± 0.1	39.7 ± 6.9
3 g	0.3 ± 0.1	0	3.2 ± 1.0	3.18 ± 0.9	46.8 ± 5.9	10.8 ± 1.7
3 h	33.7 ± 1.3	29.3 ± 2.1	42.9 ± 0.8	25.5 ± 4.0	17.5 ± 1.3	41.2 ± 1.6
3i	74.1 ± 2.3	93.8 ± 0	51.4 ± 0.1	98.1 ± 0.5	97.8 ± 0.1	85.3 ± 1.3
3j	33.3 ± 1.1	0	16.0 ± 1.1	6.2 ± 5.1	4.8 ± 0.1	33 ± 5.8
3 k	35.2 ± 2.1	53.8 ± 5.3	16.0 ± 1.1	37.8 ± 1.6	26.7 ± 1.8	59.1 ± 3.6
3 l	45.1 ± 2.1	84.6 ± 1.9	19.1 ± 1.9	86.6 ± 3.3	90.6 ± 1.3	90.1 ± 0.4
3 m	27.7 ± 4.3	0	19.1 ± 0.1	94.9 ± 0.5	63.5 ± 1.4	74.2 ± 1.9
3n	63.2 ± 1.1	40.0 ± 2.7	0.2 ± 0.1	73.3 ± 4.1	85.9 ± 1.0	73.6 ± 1.5
3o	62.6 ± 1.9	82.1 ± 2.1	50.5 ± 3.2	84.5 ± 1.2	95.0 ± 1.3	83.6 ± 0.8
3p	5.6 ± 4.8	15.4 ± 0	5.7 ± 2.8	7.8 ± 0.8	40.5 ± 0.1	14.9 ± 2.9
3q	70.4 ± 1.4	55.9 ± 1.8	17.9 ± 1.0	98.1 ± 1.4	88.9 ± 0.1	66.7 ± 0.9
3r	34.0 ± 1.9	4.1 ± 3.2	14.8 ± 2.8	30.1 ± 1.7	52.3 ± 0.1	36.2 ± 1.0
3 s	54.5 ± 2.1	53.8 ± 0.1	42.4 ± 1.0	93.8 ± 3.7	81.1 ± 1.3	84.3 ± 0.8
3 t	0.3 ± 0.1	78.0 ± 2.3	0	36.6 ± 2.9	64.3 ± 0.1	11.6 ± 0.9
3u	20.9 ± 4.3	11.8 ± 1.7	12.4 ± 0.1	83.9 ± 0.4	59.4 ± 2.5	69.1 ± 0.9
3v	1.3 ± 0.1	0	0.2 ± 0.1	15.0 ± 2.2	33.3 ± 4.8	6.2 ± 2.6
3w	17 ± 2.7	23.1 ± 0	0	28.1 ± 1.8	61.9 ± 0.1	18.1 ± 4.0
3x	34 ± 0.1	25.2 ± 1.8	8.1 ± 0.1	45.4 ± 2.4	49.3 ± 3.3	8 ± 3.7
3y	0 ± 0	16.9 ± 1.6	1.3 ± 0.1	16.5 ± 4.7	9.5 ± 4.8	10.4 ± 4.2
3z	1.3 ± 0.1	0	0	0	39.7 ± 1.4	1.6 ± 1.4
4a	22.7 ± 4.2	22.4 ± 4.0	9.3 ± 1.0	18.9 ± 1.1	2.2 ± 0.1	2.5 ± 0.1
4b	33.4 ± 1.1	92.9 ± 2.1	16.1 ± 2.1	98.4 ± 0.8	97.1 ± 1.2	78.5 ± 3.9
4c	7.8 ± 2.1	40.3 ± 2.8	1.5 ± 2.5	36.0 ± 8.1	23.9 ± 0.1	12.6 ± 3.9
4d	34.6 ± 0.1	92.9 ± 2.9	0	99.2 ± 0.8	93.5 ± 0.1	82.2 ± 1.0
4e	0	55.4 ± 1.6	1.7 ± 1.5	92.1 ± 0.9	82.9 ± 1.0	81.0 ± 0.1
4f	15.9 ± 0.1	15.4 ± 4.1	0	15.0 ± 0.1	34.8 ± 0.1	6.1 ± 2.6
5a	40.9 ± 1.2	87.8 ± 2.9	16.0 ± 1.1	93.7 ± 0.1	89.1 ± 0.1	76.1 ± 0.1
5b	27.7 ± 2.9	52.9 ± 1.3	0	29.1 ± 0.1	23.9 ± 0.1	40.5 ± 4.2
5c	27.7 ± 4.3	61.5 ± 2.0	6.9 ± 2.1	29.6 ± 0.9	29.7 ± 5.5	1.0 ± 0.2
5d	41.1 ± 1.3	60.2 ± 2.3	27.7 ± 2.7	86.8 ± 0.3	79 ± 1.2	75.5 ± 1.1
5e	20.6 ± 3.9	40.3 ± 2.8	0	38.9 ± 6.7	52.3 ± 0.1	1.8 ± 1.0
boscalid	44.2 ± 1.6	75.3 ± 2.0	49.4 ± 3.2	100.0 ± 0.0	91.8 ± 1.3	91.7 ± 1.4

^a Values are the mean ± standard deviation (SD) of three replicates.

ble to boscalid. However, compounds **3i** and **3q** showed lower inhibitory activity against *S. sclerotiorum* than boscalid ($EC_{50} = 0.393$ and 0.128 mg/L, respectively).

For *G. zeae*, compounds **3i** and **3l** exhibited good antifungal activity with the EC_{50} value of 1.10 and 1.55 mg/L, respectively. For *B. cinerea*, compounds **3i**, **4b** and **4d** (greater than 90 % mycelial growth inhibition) were examined for EC_{50} values. In result, **3i** displayed excellent antifungal activity ($EC_{50} = 0.199$ mg/L), which was much stronger than boscalid ($EC_{50} = 1.41$ mg/L). Compounds **4b** and **4d** also displayed good inhibition to *B. cinerea*, which was approached to boscalid. As for *A. solani*, compounds **3i** and **4b** showed good activity ($EC_{50} = 0.154$ mg/L and 0.323 mg/L, respectively), which were equipotent to boscalid ($EC_{50} = 0.117$ mg/L). As for *R. solani*, only compounds **3q** and **3i** showed better antifungal inhibition than boscalid, with $EC_{50} = 0.154$ mg/L and

0.323 mg/L, respectively. In general, compounds **3i** and **4b** displayed broad spectrum of antifungal activity toward the test fungi.

In addition, to visualize the inhibitory effect, the mycelium growth of *S. sclerotiorum* on PDA medium plates containing five concentrations of compound **4b** was presented in Fig. 2. In result, the hyphae growth and extension of *S. sclerotiorum* were dramatically restricted in a concentration-dependent manner. In particular at 0.049 mg/L, compound **4b** displayed 42.8 % inhibition to mycelia growth, which was superior over boscalid (35.2 % inhibition). Even under the lower dosage (0.012 mg/L), compound **4b** could also moderately inhibit the mycelium growth (32.2 % inhibition), whereas boscalid displayed only 10.0 % inhibition. The results indicated that the compounds were endowed with perceptible antifungal competency.

Table 2 In vitro EC₅₀ of selected compounds against six kinds of pathogenic fungi.

fungi	compd	EC ₅₀ (mg/L)	regression equation	R ²	Confidence Interval 95 %
<i>S. sclerotiorum</i>	3i	0.393	y = 1.77 × + 0.718	0.933	0.145–1.34
	3q	0.128	y = 1.63 × + 1.45	0.981	0.021–0.548
	4b	0.067	y = 1.30 × + 1.53	0.984	0.044–0.096
	4d	0.092	y = 2.19 × + 2.27	0.953	0.071–0.118
	boscalid	0.118	y = 1.92 × + 1.79	0.978	0.089–0.154
<i>G. zeae</i>	3i	1.10	y = 1.31 × − 0.054	0.924	0.742–1.81
	3l	1.55	y = 1.16 × − 0.219	0.969	0.97–2.91
	boscalid	0.431	y = 1.98 × + 0.723	0.942	0.331–0.569
<i>B. cinerea</i>	3i	0.199	y = 1.70 × + 1.19	0.986	0.148–0.267
	4b	2.18	y = 1.44x − 0.486	0.943	1.43–3.84
	4d	1.63	y = 1.31 × − 0.276	0.948	1.06–2.85
	boscalid	1.41	y = 2.52 × − 0.377	0.988	0.811–3.10
<i>A. solani</i>	3i	0.154	y = 1.92 × − 1.55	0.998	0.117–0.202
	3o	0.248	y = 2.03 × − 1.23	0.943	0.089–0.737
	4b	0.323	y = 1.93 × + 0.947	0.938	0.138–0.837
	boscalid	0.117	y = 1.90 × + 1.77	0.991	0.089–0.154
<i>R. solani</i>	3i	6.54	y = 1.72 × − 1.40	0.979	2.34–11.8
	3q	4.41	y = 1.10 × − 0.709	0.957	3.84–15.3
	boscalid	greater than50	/	/	/

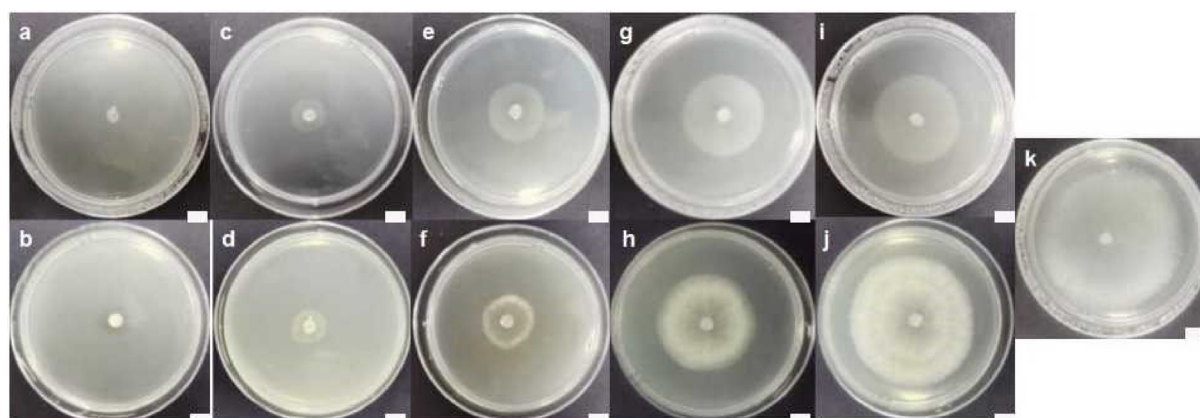


Fig. 2 Mycelium growth and extension of *S. sclerotiorum* after treatment with different concentrations of compound **4b** on agar medium: (a) 3.125; (c) 0.781; (e) 0.195; (g) 0.049; (i) 0.012 and (k) 0 mg/L; Boscalid on agar medium: (b) 3.125; (d) 0.781; (f) 0.195; (h) 0.049; and (j) 0.012 mg/L (25 °C for 2 d). The scale bars in all graphs were 1.0 cm.

3.3. SAR discussion

As illustrated in Table 1, among series **3a-3z**, compounds could be divided as derivatives with single heterocycles (**3a-3s**) and derivatives with benzo-heterocycles (**3t-3z**). Notably, compounds with pyrazole (**3i**), thiazole (**3l** and **3m**), isoxazole (**3o**) and furan (**3q**) group demonstrated good antifungal activities against one or more fungal strains, which were better than most compounds with six-member rings (pyridine and phenyl ring) (i.e. **3a-3d**, **3f** and **3g**). For instance, compound **3i** displayed more than 90 % inhibition rates against *B. cinerea*, *S. sclerotiorum*, and *A. solani*, which were comparable to boscalid. In contrast, other compounds with benzo-heterocycles fragments (**3t-3z**) exhibited weak to moderate antifungal activity against several tested fungi, which were quite inferior to the derivatives with single heterocycles. In additions, the other

type of compounds, which contained the benzene-heterocyclic fragments (**4a-4f**), displayed different extent antifungal activities against six test fungi. In detail, compound **4b** with 2-phenyl-thiazole moiety exhibited prominent antifungal activity toward *S. sclerotiorum*, *B. cinerea* and *A. solani*, which were much stronger than compounds with 3-phenylpyrazole and 3-phenylisoxazole moieties (**4a** and **4c**). Meanwhile, compounds **4d** and **4e** containing pyrazole-phenyl and 1,2,4-oxadiazole-phenyl moieties also displayed strong activities to several fungal strains, while **4f** with thiophene-isoxazole moiety only showed very weak activity. These results indicated that different combinations of two aromatic rings had significant effect on antifungal activity.

Moreover, the substituents on aromatic rings could exert substantial effect the antifungal activity. For example, as for series **5**, compound **5a** with electron withdrawing 4-fluoro

group on 2-phenoxyacetamide moiety showed stronger anti-*S. sclerotiorum* activity and anti-*A. solani* activity than compounds **5b-5e**. For other series, the derivatives (**3e**, **3i**, **3n** and **4e**) with electron withdrawing group such as CF₃ generally displayed much better antifungal activities than the derivatives (**3f** and **5c**) with electron donating OCH₃ group. In addition, compound **3e** with 4-CF₃-pyridine exhibited stronger activity than 2-CF₃-pyridine derivative **3d**, suggesting that the position of substituents could also affect the antifungal activity to some extent.

In brief, it could make the conclusion that among these aromatic carboxamides from dehydroabietylamine, compounds contained with five member-rings, 2-phenyl-thiazole or pyrazole-phenyl moieties displayed more potent antifungal activities than compounds with six member-rings, phenylpyrazole or 3-phenylisoxazole moieties. The electron-withdrawing substituents on heterocycles were generally more beneficial to the antifungal activity than the electron-donating ones.

3.4. *In vivo* bioassay on rape leaves infected by *S. sclerotiorum*.

The active compound **4b** was further evaluate for the protective effects against *S. sclerotiorum* infected-rape leaves. The efficacy of the treatment was presented in Fig. 3 and Table 3. Compound **4b** displayed strong protective effects at 200 mg/L, which was active at the same level with boscalid (100 %). Even under low dosage (100 mg/L), **4b** still demonstrated good protective effects toward *S. sclerotiorum*. These observations indi-

cated that compound **4b** exhibited prominent protective effects *in vivo* with broad chance of structure modification and optimization for further development.

3.5. *In vivo* bioassay on tomato plants infected by *B. cinerea*.

The *in vivo* anti-*B. cinerea* activity of three compounds **3i**, **4b** and **4d** on tomato plants were further evaluated in greenhouse experiments. The results was presented in Fig. 4 and Table 4. Compound **3i** and **4d** displayed pronounced inhibitory effect toward *B. cinerea*, with the control efficacies of 86.0 % and 89.0 %, respectively, which were approached to boscalid (95.0 %). In addition, compound **4b** also afforded notable effectiveness of 78.0 % against *B. cinerea*. In summary, the compound **3i** and **4d** could effectively control the fungal infection on tomato plants.

3.6. Sclerotia formation inhibition Assay.

Sclerotia, which served as the initial inoculum in the *S. sclerotiorum* infection process, could survive for several years in soil under adverse environmental conditions. Therefore, inhibition of sclerotia formation plays a key role in controlling *S. sclerotiorum*. As could be seen in Fig. 5B, compound **4b** exhibited a good inhibition effect on the sclerotia formation (95.2, 60.6, and 15.1 % inhibition) comparable to that of boscalid (Fig. 5C, 100, 50.6, and 28.1 % inhibition) at 0.2, 0.1, and 0.05 mg/L, respectively.

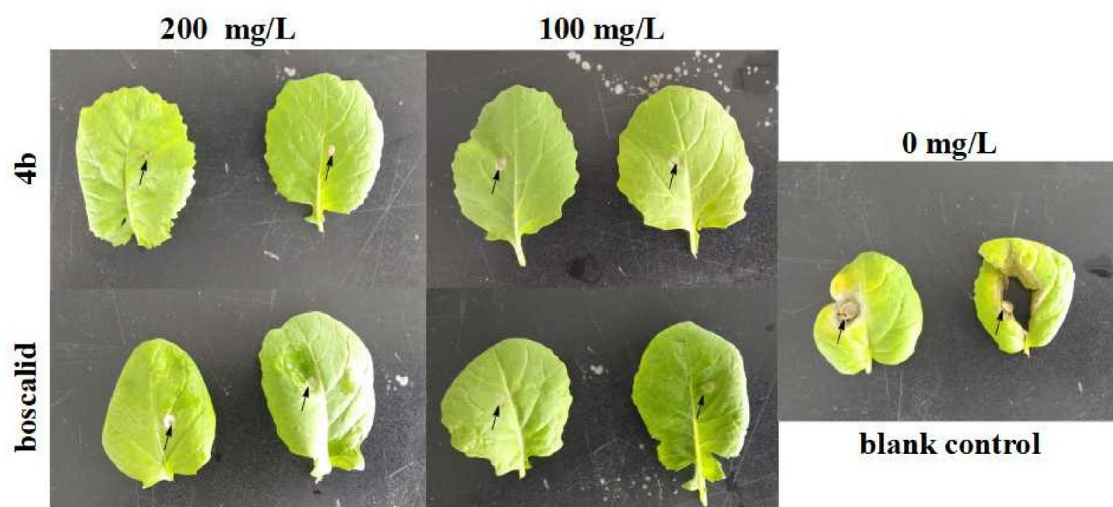


Fig. 3 *In vivo* protective effects of compound **4b** on rape leaves infected by *S. sclerotiorum*^a.

Table 3 *In vivo* protective effects of compound **4b** on rape leaves infected by *S. sclerotiorum*.^a

Compd.	Treatment (mg/L)	Diameter lesion length (mm)	Protective activity ^a (%)
4b	200	5.0 ± 0.06	100
	100	5.0 ± 0.07	100
Boscalid	200	5.0 ± 0.05	100
	100	5.0 ± 0.1	100
Negative Control	0	27.5 ± 0.398	/

^a Values are the average of nine replicates.



Fig. 4 *In vivo* antifungal activity of compounds **3i**, **4b** and **4d** to *B. cinerea*-infected tomato plants in greenhouse experiment.

Table 4 *In vivo* antifungal effects of compounds **3i**, **4b** and **4d** on tomato plants infected by *B. cinerea*.

Compd.	Disease index	Control efficacy (%)
3i	4.0 ± 0.60 ^a	86.0
4b	6.0 ± 1.91 ^a	78.0
4d	3.0 ± 0.98 ^a	89.0
boscalid	1.0 ± 0.04 ^a	95.0
Negative Control	29 ± 7.89 ^b	/

The letters a–b denoted the results of difference significance analysis. Means followed by the same letter within the same column are not significantly different (p greater than 0.05, Fisher's LSD multiple comparison test).

3.7. Effect of compound **4b** on exopolysaccharide of *S. Sclerotiorum* strains

Exopolysaccharide is a major component for the growth of fungal cells. The exopolysaccharide mass of the mycelia in the blank control was 0.685 mg/mL (Fig. 6). After treatment with compound **4b**, the exopolysaccharide content was reduced, especially at 0.2 mg/L group (exopolysaccharide content 0.125 mg/mL). These results indicated that **4b** could concentration-dependently reduce the formation of exopolysaccharide of *S. sclerotiorum*.

3.8. SEM analysis

Compound **4b** with the best EC₅₀ (0.067 mg/L) was selected for SEM analysis. The mycelia of *S. sclerotiorum* were treated with **4b** and boscalid at three concentrations of 0.195 mg/L (Fig. 7e, f), 0.781 mg/L (Fig. 7c, d) and 3.125 mg/L (Fig. 7a, b). The structural changes of mycelia were observed through SEM. As a result, the mycelia of the sample without treatment of **4b** were regular and smooth in surface, and present an intact structure (Fig. 7g). In contrast, the structure of mycelia treated with **4b** were shrunk at 0.195 and 0.781 mg/L (Fig. 7e, c).

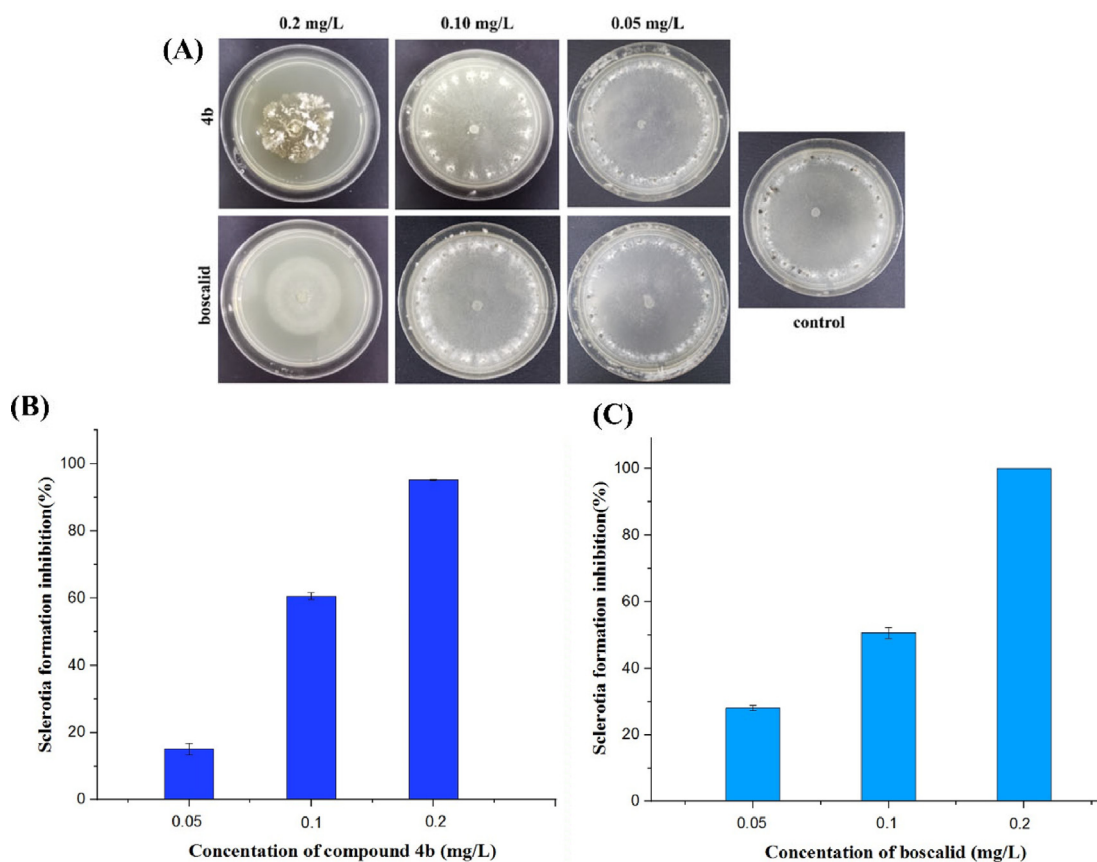


Fig. 5 Effect of compound **4b** (A, B) and boscalid (A, C) on the sclerotia formation.

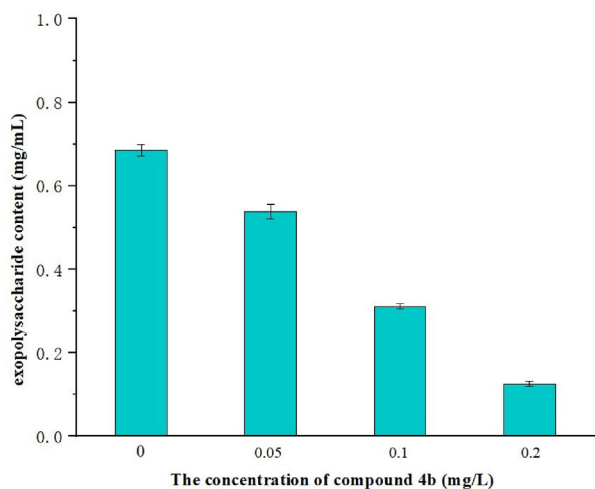


Fig. 6 Effect of compound **4b** on exopolysaccharide of *S. sclerotiorum* strains.

Moreover, drastic changes in mycelial morphology were observed. And the mycelia presented noticeable shrinkage and different extent of distortion after treating with **4b** at 3.125 mg/L (Fig. 7a). However, when treated with boscalid

at 0.195 and 0.781 mg/L, the mycelia were not notably crumpled and shriveled. Only at 3.125 mg/L (Fig. 7b), the mycelial morphology was seriously injured, which was comparable to the effect of **4b** at the same dosage. This result revealed that **4b** had a strong capacity to damage the surface morphology of mycelia and seriously interfere with the growth and reproduction of *S. sclerotiorum* strain.

3.9. TEM analysis

As for the TEM observation, the mycelium cells in the blank control group (Fig. 8A) had complete structure, with uniform cytoplasm, the cell wall (CW), plasma membrane (PM), mitochondria and other organelles are clearly visible. After treatment with compound **4n**, the structure of the cells were damaged, the cell wall became thickened and the mitochondria (M) even disappeared (Fig. 8B). These results indicated that compound **4b** had an excellent ability to destroy the ultrastructure of hyphae cells.

3.10. Cell cytotoxicity assay

Two selected compounds with high antifungal activity and SDH inhibitory activity were evaluated on their cytotoxicity to A549 cells. As illustrated in Table 5, the viability of A549 cells treated by compounds **4b** and **4d** at 10 μ M were comparable to boscalid. In addition, compounds **4b** and **4d** exhibited

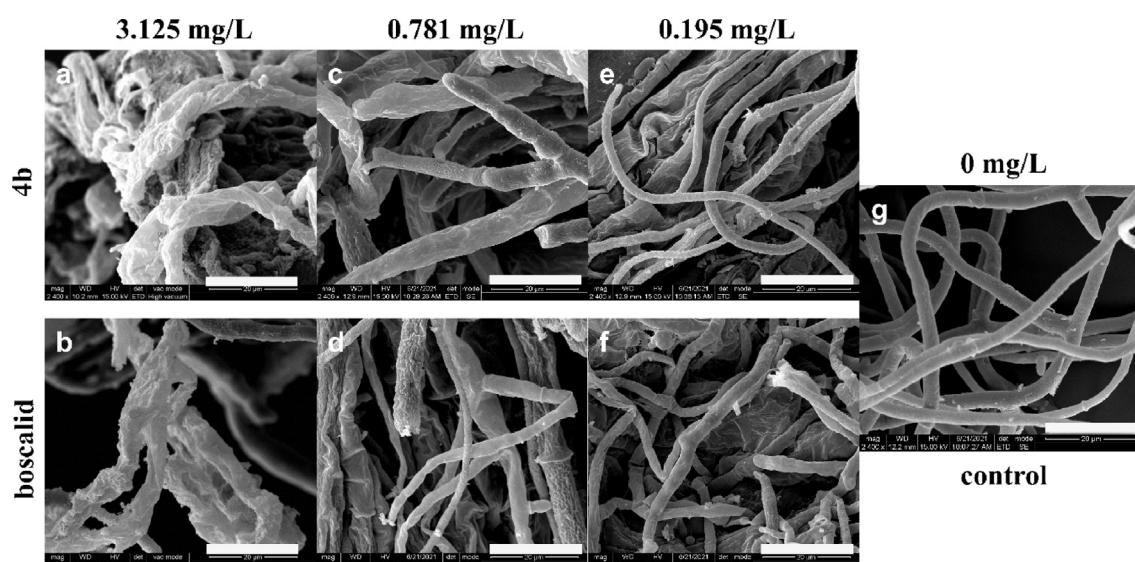


Fig. 7 Scanning electron micrographs of *S. sclerotiorum* hyphae in the untreated control (g) and (a) 3.125 mg/L, (c) 0.781 mg/L, (e) 0.195 mg/L of compound **4b**; (b) 3.125 mg/L, (d) 0.781 mg/L, (f) 0.195 mg/L of positive control boscalid. The scale bars of graphs a-g were 20 μ m.

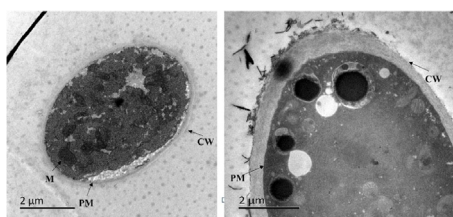


Fig. 8 TEM observation of the cellular structure of *S. sclerotiorum* (A) DMSO control and (B) compound **4b** at 0.067 mg/L, the scale bar of graphs was 2 μ m.

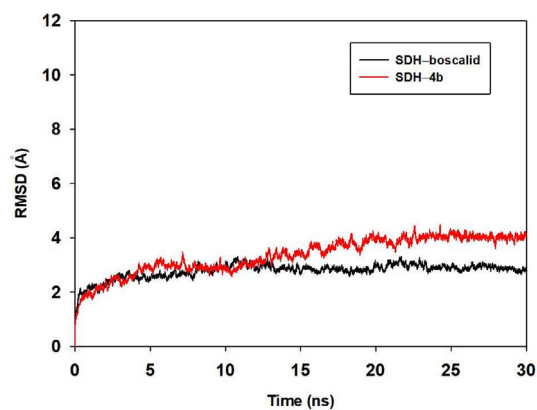


Fig. 9 The root-mean-square deviations (RMSDs) of all the atoms of SDH-**4b** complex and SDH-boscalid complex during the 30 ns simulation.

compd	A549 cell	
	Cell viability (%)	IC ₅₀ (μ M)
4b	89.6	91.1
4d	88.2	86.3
boscalid	92.5	86.7

compd	IC ₅₀ (μ M)	regression equation	r ²
3i	46.5 \pm 0.5	y = 2.11 x-3.51	0.933
3q	49.1 \pm 0.9	y = 2.47 x-4.17	0.989
4b	23.3 \pm 1.6	y = 2.68 x-3.66	0.979
4d	28.9 \pm 3.7	y = 1.79 x-2.62	0.992
boscalid	6.14 \pm 0.8	y = 1.56 x-1.23	0.910

substantially low cytotoxicity (IC₅₀ = 91.1 μ M and 86.3 μ M, respectively), which were also comparable to boscalid (IC₅₀ = 86.7 μ M). On the whole, by comparing with boscalid, compounds **4b** and **4d** displayed sufficient safety and exhibited the potential for the development of fungicides.

3.11. In vitro SDH inhibition assay

Compounds **3i**, **3q**, **4b** and **4d** exhibited moderate to good SDH inhibition with IC₅₀ values ranging in 20 ~ 50 μ M (Table 6). Among them, compound **4b** exhibited the highest inhibitory activity with IC₅₀ value of 23.3 \pm 1.6 μ M. In addition, compounds **4d**, **3i** and **3q** also exhibited moderate to good inhibitory activities. These results suggested that the inhibition of

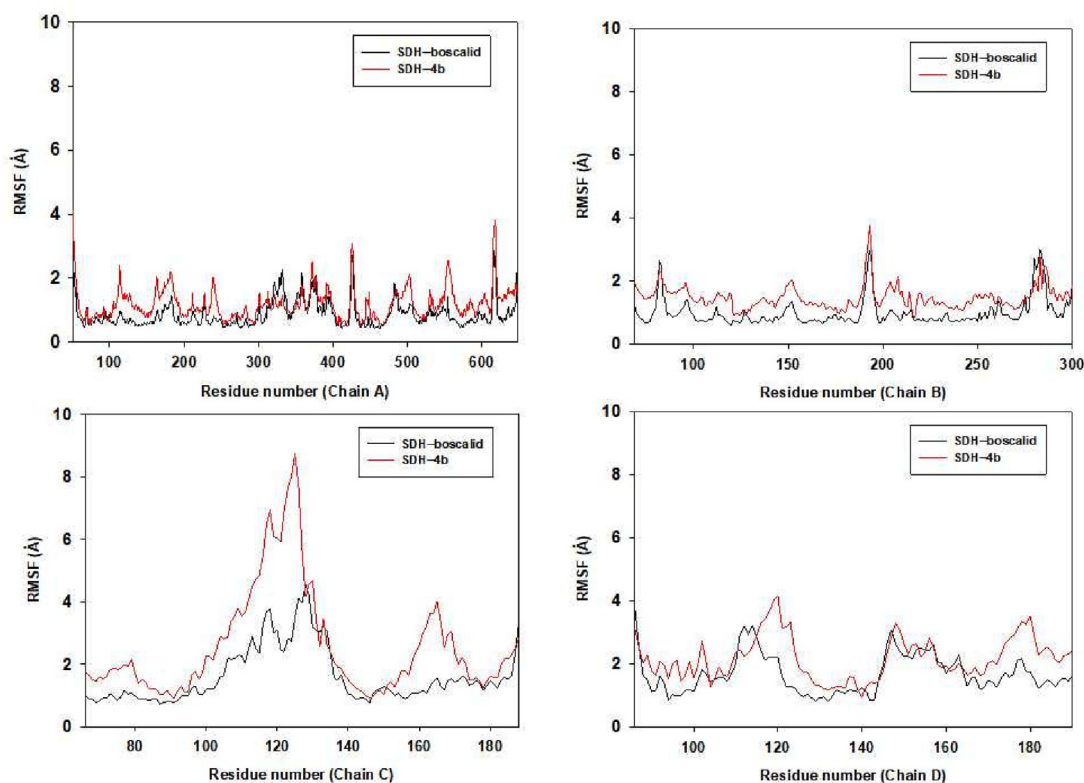


Fig. 10 The RMSFs of residues of the whole protein in complexes SDH-**4b** and SDH-boscalid during the 30 ns simulation.

SDH could be potential mechanism for the title compounds as fungicides.

3.12. MDS study

According to the SDH inhibition results, the binding mechanism of SDH with **4b** and boscalid were further explored. First, the MDS study was carried out. Besides, the RMSD values of the protein backbone were calculated and plotted for investigating the dynamic stability of SDH-**4b** complex and SDH-boscalid complex. It was observed that the protein structures of the two systems were stabilized during the 30-ns simulation (Fig. 9).

Subsequently, RMSF for residues of protein in both SDH-**4b** and SDH-boscalid complex were also calculated (Fig. 10), which described various flexibilities in the binding pocket of SDH when **4b** and boscalid were present. Furthermore, in the binding pocket of SDH, most of the amino acid residues interacting with **4b** and boscalid also exhibited small flexibility with $\text{RMSF} < 2 \text{ \AA}$, indicating that residues would be more rigid as a result of binding with **4b** and boscalid.

The per residue interaction free energies contained four parts, including *Van der Waals* (ΔE_{vdw}), solvation (ΔE_{sol}), electrostatic (ΔE_{ele}) and total contribution (ΔE_{total}) (Fig. 11). In the SDH-**4b** complex, the D/Arg-154 residue has an excellent electrostatic (ΔE_{ele}) contribution (Fig. 11a). Detailed data

analysis displayed that the D/Arg-154 residue was approached to **4b** via two hydrogen bond interactions (bond lengths: 3.2 Å and 3.5 Å) (Fig. 12a). Besides, the B/Trp-230 and D/Tyr-144 residues (Fig. 11a) have an appreciable *Van der Waals* (VDW) interactions with **4b** (Fig. 12a). In additions, decomposed energy interaction originated from VDW interactions, apparently through hydrophobic interactions. On the other hand, the D/Asp-143 residue has moderate electrostatic (ΔE_{ele}) contribution, with the ΔE_{ele} of $< -2.5 \text{ kcal/mol}$ (Fig. 12b) in SDH-boscalid complex. This analysis revealed that the D/Asp-143 residue was adjacent to phenyl group of boscalid, forming the anion- π interaction (Fig. 12b). Besides, the residue B/Pro-226 (ΔE_{vdw} of $< -2.0 \text{ kcal/mol}$), have an appreciable VDW interactions with the boscalid because of the close proximity between the residue and the boscalid (Fig. 12b). With the exception of the B/Pro-226 and D/Asp-143 residues, the decomposed energy interaction originated from VDW interactions, obviously through hydrophobic interactions (i.e. B/Trp-229, B/Trp-230, B/Ile-275, C/Leu-72, C/Trp-81, C/Ile-82, C/Leu-86 and C/Phe-87). Moreover, total binding free energy of two complexes were calculated according to the MMGBSA approach, and the ΔG_{bind} values were found for **4b** (-42.6 kcal/mol) and boscalid (-32.1 kcal/mol), which demonstrated that **4b** could form a tight interaction with SDH.

In brief, MDS study offered effective clues and reasonable analysis of binding mechanism of SDH with **4b** and boscalid,

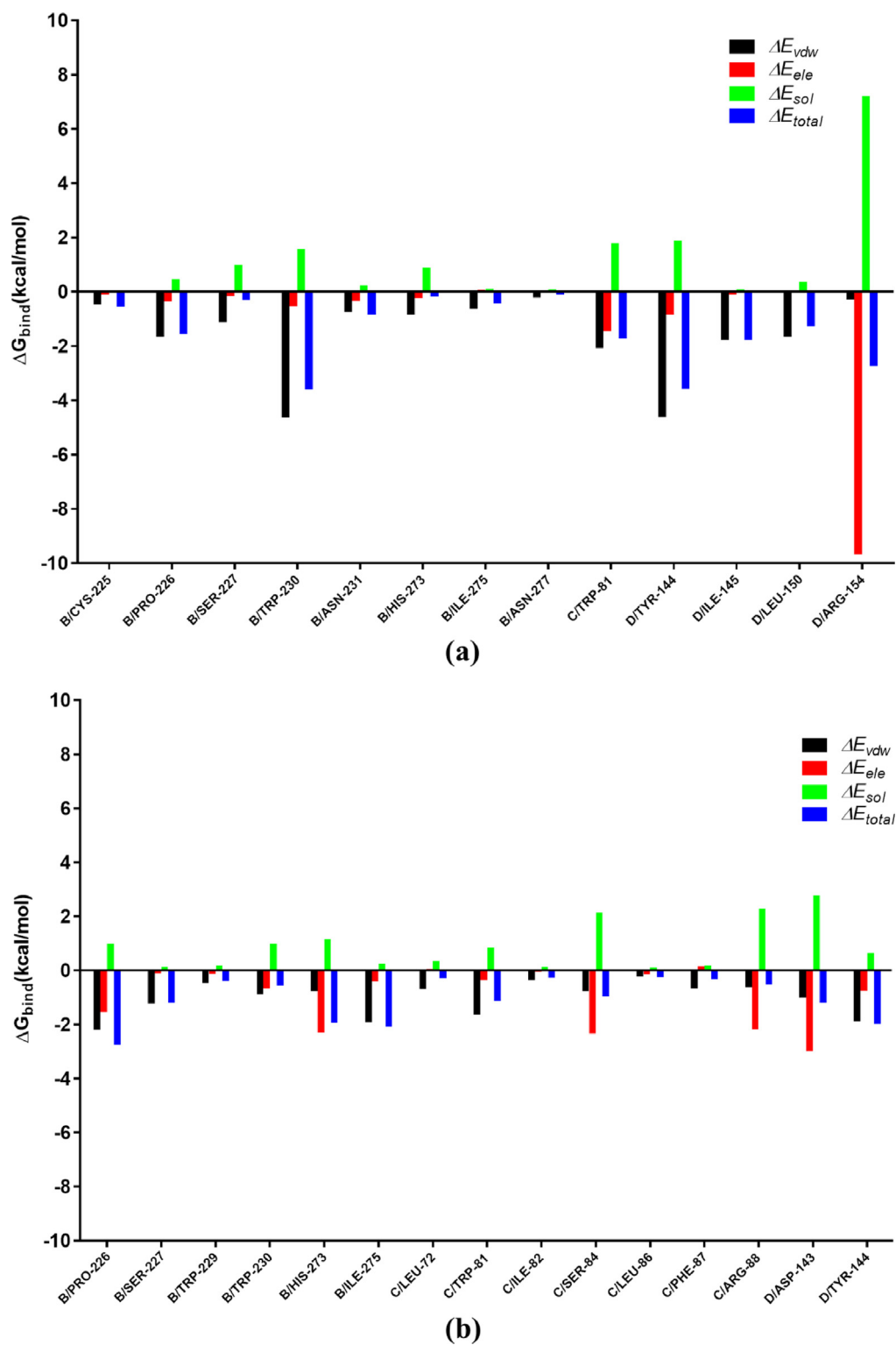


Fig. 11 Decomposition of the binding energy on a per-residue basis in complex SDH-4b (a) and complex SDH-boscalid (b).

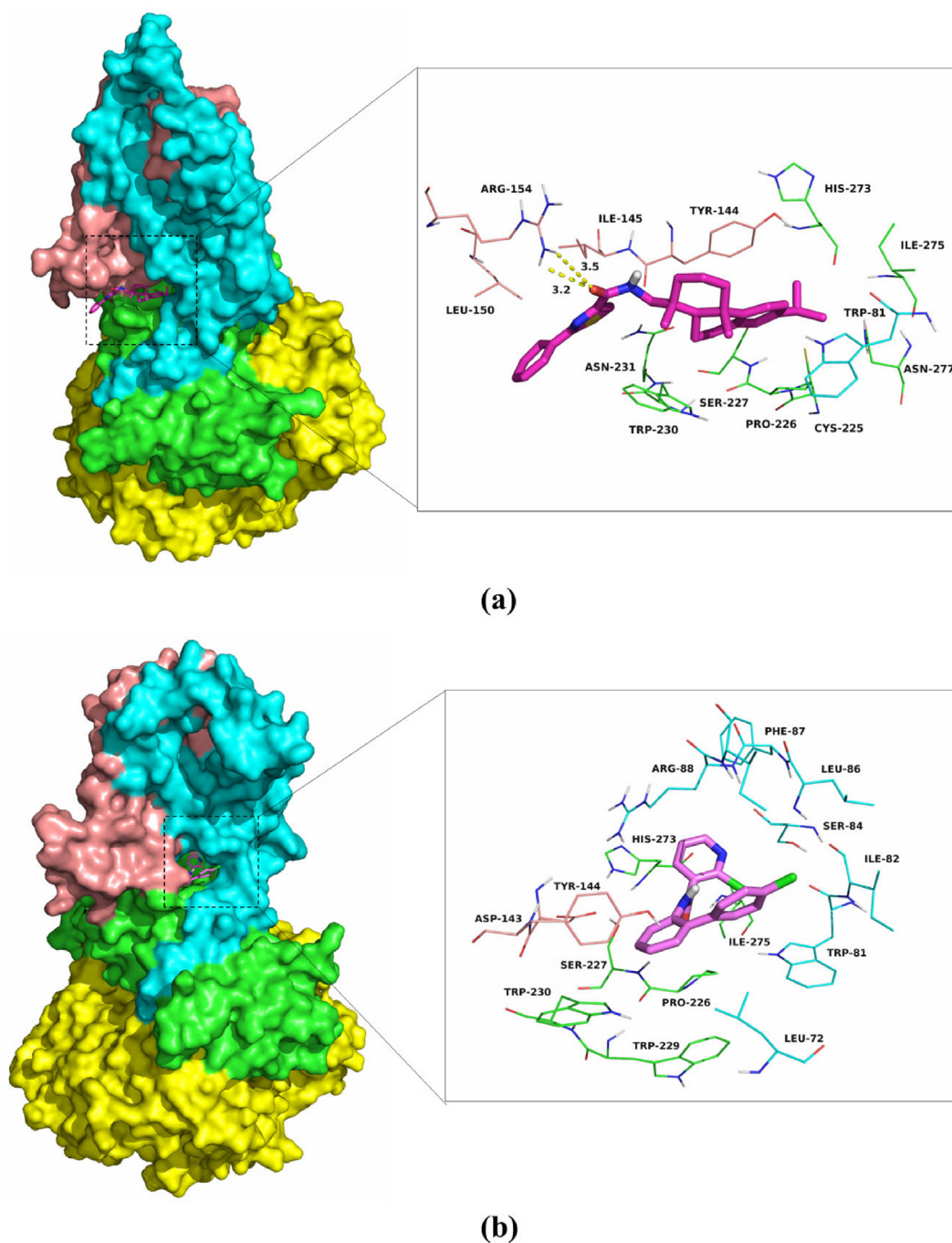


Fig. 12 The predicted binding modes of compound **4b** (a) and boscalid (b) in SDH binding pockets obtained from molecular dynamics simulation (chains A, B, C and D of SDH were colored by yellow, cyan, green and salmon, respectively; compound **4b** and boscalid were shown in rose red and pink sticks, respectively).

which could give the preliminary conduction for the discovery of novel fungicides.

4. Conclusions

In this work, 37 heterocyclic carboxamide derivatives of dehydroabietylamine were synthesized and characterized. *In vitro* test displayed that most of the synthesized compounds demonstrated moderate to

excellent antifungal activities toward six phytopathogenic fungi. Compounds **3i**, **3q**, **4b** and **4d** showed significant antifungal activity toward *S. sclerotiorum*, and compounds **3i**, **4b** and **4d** also displayed prominent antifungal activity toward *B. cinerea* with EC_{50} values comparable to boscalid. In the *in vivo* antifungal assay, compound **4b** exhibited brilliant protective activity against *S. sclerotiorum*-infected rape leaves. The *in vivo* antifungal bioassay on tomato plants demonstrated that compound **3i** and **4d** displayed excellent anti-*B. cinerea* efficacy at

200 mg/L, which were comparable to boscalid. In the antifungal mechanism study, compound **4b** could dose-dependently inhibit the sclerotia formation and reduce the exopolysaccharide level of *S. sclerotiorum*. The SEM and TEM analyses revealed that **4b** could injure the morphological integrity and the cell ultrastructure of *S. sclerotiorum* mycelia. Furthermore, compound **4b** and **4d** presented good inhibitory activity against SDH. Molecular modeling suggested that compound **4b** could bind well with the active site of SDH. These works indicated that this type of compounds could be considered as effective candidates for the new fungicides development.

Declaration of Competing Interest

The authors declare that they have no known competing interest financial interest or personal relationships that could have appeared to influence the work reported in this paper.

Acknowledgments

This work was supported by the National Natural Science Foundation of China (No. 31770616) and the Natural Science Foundation for Colleges and Universities in Jiangsu Province of China (No. 17KJA220002).

Appendix A. Supplementary material

Supplementary data to this article can be found online at <https://doi.org/10.1016/j.arabjc.2022.104330>.

References

- Brown, J.K.M., 2002. Aerial dispersal of pathogens on the global and continental scales and its impact on plant disease. *Science* 297, 537–541.
- Cai, X.M., Tang, Z.G., Chen, X.F., Lin, Y.T., Zhang, X.D., Huang, S.L., 2022. Construction of two rosin-based BioAIEgens with distinct fluorescence and mechanochromic properties for rewritable paper. *Dyes Pigm.* 204, 110454.
- Chen, N.Y., Duan, W.G., Lin, G.S., Liu, L.Z., Zhang, R., Li, D.P., 2016. Synthesis and antifungal activity of dehydroabietyl acid-based 1,3,4-thiadiazole-thiazolidinone compounds. *Mol. Divers.* 20, 897–905.
- Chen, Y.H., Yeh, T.F., Chu, F.H., Hsu, F.L., Chang, S.T., 2015. Proteomics investigation reveals cell death-associated proteins of Basidiomycete Fungus *Trametes versicolor* treated with ferruginol. *J. Agric. Food Chem.* 63, 85–91.
- Cheng, W., Yan, Y.K., Xiao, T.T., Zhang, G.L., Zhang, T.T., Lu, T., Jiang, W.J., Wang, J.W., Tang, X.R., 2021. Design, synthesis and inhibitory activity of novel 2,3-dihydroquinolin-4(1H)-one derivatives as potential succinate dehydrogenase inhibitors. *Eur. J. Med. Chem.* 214, 113246.
- da Silva, A.W.S., Vranken, W.F., 2012. ACPYPE-Antechamber python parser interface. *BMC Res. Notes.* 5, 367.
- Dea-Ayuela, M.A., Bilbao-Ramos, P., Bolas-Fernandez, F., Gonzalez-Cardenete, M.A., 2016. Synthesis and antileishmanial activity of C7-and C12-functionalized dehydroabietylamine derivatives. *Eur. J. Med. Chem.* 121, 445–450.
- Fei, B.L., Hui, C.N., Wei, Z.Z., Kong, L.Y., Long, J.Y., Qiao, C.H., Chen, Z.F., 2021. Copper(II) and iron(III) complexes of chiral dehydroabietyl acid derived from natural rosin: metal effect on structure and cytotoxicity. *Metallomics* 13, mfab014.
- Fishel, F.M., Dewdney, M.M., 2015. Fungicide Resistance Action Committee's (FRAC) Classification Scheme of Fungicides According to Mode of Action. Miami-Dade County, Florida.
- Fisher, M.C., Henk, D.A., Briggs, C.J., Brownstein, J.S., Madoff, L.C., Mccraw, S.L., Gurr, S.J., 2012. Emerging fungal threats to animal, plant and ecosystem health. *Nature* 484, 186–194.
- Gao, Y.Q., Wang, Y., Li, J., Shang, S.B., Song, Z.Q., 2018. Improved application of natural forest product terpene for discovery of potential botanical fungicide. *Ind. Crop. Prod.* 126, 103–112.
- Götz, A.W., Williamson, M.J., Xu, D., Poole, D., Le, G., S., Walker, R.C., 2012. Routine microsecond molecular dynamics simulations with AMBER on GPUs. I. Generalized Born. *J. Chem. Theory Comput.* 8, 1542–1555.
- Guo, X.F., Zhao, B., Fan, Z.J., Yang, D.Y., Zhang, N.L., Wu, Q.F., Yu, B., Zhou, S., Kalinina, T.A., Belskaya, N.P., 2019. Discovery of novel thiazole carboxamides as antifungal succinate dehydrogenase inhibitors. *J. Agric. Food Chem.* 67, 1647–1655.
- Jin, H., Zhou, J., Pu, T., Zhang, A., Zhou, J., Pu, T., Zhang, A., Gao, X., Tao, K., Hou, T., 2017. Synthesis of novel fenfuram-diarylether hybrids as potent succinate dehydrogenase inhibitors. *Bioorg. Chem.* 73, 76–82.
- Kusumoto, N., Ashitani, T., Murayama, T., Ogiyama, K., Takahashi, K., 2010. Antifungal abietane-type diterpenes from the cones of *Taxodium distichum* Rich. *J. Chem. Ecol.* 36, 1381–1386.
- Liang, P.B., Shen, S., Xu, Q., Wang, S.M., Jin, S.H., Lu, H.Z., Dong, Y.H., 2021. Design, synthesis biological activity, and docking of novel fluopyram derivatives containing guanidine group. *Bioorg. Med. Chem.*, 115846.
- Liu, C.X., Lin, Z.X., Lu, Z., Wang, Y.M., Bao, Y.L., 2013. Antitumor and scavenging radicals activities of some polyphenols related to dehydroabietylamine derivatives. *J. Asian Nat. Prod. Res.* 15, 819–827.
- Liu, M., Liu, Y., Zhou, S., Zhang, X., Yu, S., Li, Z., 2016. Synthesis and antifungal activities of novel strobilurin derivatives containing quinolin-2(1H)-one moiety. *Chem. Res. Chin. Univ.* 32, 600–606.
- Liu, X.H., Qiao, L., Zhai, Z.W., Cai, P.P., Cantrell, C.L., Tan, C.X., Weng, J.Q., Han, L., Wu, H.K., 2019. Novel 4-pyrazole Carboxamide Derivatives Containing Flexible Chain Motif: Design, Synthesis and fungicidal Activity. *Pest. Manage. Sci.* 75, 2892–2900.
- Liu, H., Xia, D.G., Hu, R., Wang, W., Cheng, X., Wang, A.L., Zhang, Q., Lv, X.H., 2020. Bioactivity-oriented modification strategy for SDH inhibitors with superior activity against fungal strains. *Pestic. Biochem. Physiol.* 163, 271–279.
- Lu, T., Yan, Y.K., Zhang, T.T., Zhang, G.L., Xiao, T.T., Cheng, W., Jiang, W.J., Wang, J.W., Tang, X.R., 2021. Design, Synthesis, Biological Evaluation, and Molecular Modeling of Novel 4H-Chromene Analogs as Potential Succinate Dehydrogenase Inhibitors. *J. Agric. Food Chem.* 69, 10709–10721.
- Mao, S.Y., Wu, C.Y., Gao, Y.Q., Hao, J., He, X.H., Tao, P., Li, J., Shang, S.B., Song, Z.Q., Song, J., 2021. Pine rosin as a valuable natural resources in the synthesis of fungicides candidates for controlling *Fusarium Oxysporum* on cucumber. *J. Agric. Food Chem.* 69, 6475–6484.
- Mitani, S., Araki, S., Yamaguchi, T., Takii, Y., Ohshima, T., Matsuo, N., 2001. Antifungal activity of the novel fungicide cyazofamid against phytophthora infestans and other plant pathogenic fungi *in vitro*. *Pestic. Biochem. Physiol.* 70, 92–99.
- Morris, G.M., Huey, R., Lindstrom, W., Sanner, M.F., Belew, R.K., Goossell, D.S., Olson, A.J., 2009. AutoDock4 and AutoDockTools4: Automated docking with selective receptor flexibility. *J. Comput. Chem.* 30, 2785–2791.
- Nian, S.Y., Yu, Z.P., Tan, X.D., Gan, X., Huang, M.H., Zhou, Y.H., Wang, G.P., 2018. Synthesis and biological evaluation of *N*-(5-(2,5-dimethyl-phenoxy)-2,2-dimethylpentyl)-benzamide derivatives as novel farnesoid X receptor (FXR) antagonist. *Lett. Drug Des. Discovery.* 15, 923–936.
- Pennisi, E., 2010. Armed and dangerous. *Science* 327, 804–805.
- Pierce, L.C., Salomon-Ferrer, R., Augusto, F., de Oliveira, C., Andrew McCammon, J., Walker, R.C., 2012. Routine access to millisecond

- time scale events with accelerated molecular dynamics. *J. Chem. Theory Comput.* 8, 2997–3002.
- Roa-Linares, V.C., Brand, Y.M., Agudelo-Gomez, L.S., Tangarife-Castano, V., Betancur-Galvis, L.A., Gallego-Gomez, J.C., Gonzalez, M.A., 2016. Anti-herpetic and anti-dengue activity of abietane ferruginol analogues synthesized from (+)-dehydroabietylamine. *Eur. J. Med. Chem.* 108, 79–88.
- Sadashiva, M.P., Gowda, R., Wu, X.Z., Inamdar, G.S., Kuzu, O.F., Rangappa, K.S., Robertson, G.P., Gowda, D.C., 2015. A non-cytotoxic N-dehydroabietylamine derivative with potent antimalarial activity. *Exp. Parasito.* 155, 68–73.
- Salehi, P., Ayyari, M., Bararjanian, M., Ebrahimi, S.N., Aliahmadi, A., 2014. Synthesis, antibacterial and antioxidant activity of novel 2,3-dihydroquinazolin-4(1H)-one derivatives of dehydroabietylamine diterpene. *J. Iran Chem. Soc.* 11, 607–613.
- Salomon-Ferrer, R., Götz, A.W., Poole, D., Le, G., S., Walker, R.C., 2013. Routine microsecond molecular dynamics simulations with Amber on GPUs. 2. Explicit solvent particle mesh Ewald. *J. Chem. Theory Comput.* 9, 3878–3888.
- Sanner, M.F., 1999. Python: a programming language for software integration and development. *J. Mol. Graph. Model.* 17, 57–61.
- Sun, F., Huo, X., Zhai, Y., Wang, A., Xu, J., Su, D., Bartlam, M., Rao, Z., 2005. Crystal structure of mitochondrial respiratory membrane protein complex II. *Cell* 121, 1043–1057.
- Syngenta Crop Protection AG, Research and Development, Switzerland, 2020. FRAC classification on mode of action. Mode of action of fungicides. <http://www.frac.info/> (accessed on 2020).
- Tao, P., Wu, C.Y., Hao, J., Gao, Y.Q., He, X.H., Li, J., Shang, S.B., Song, Z.Q., Song, J., 2020. Antifungal application of rosin derivatives from renewable pine resin in crop protection. *J. Agric. Food Chem.* 68, 4144–4154.
- Trott, O., Olson, A.J., 2010. AutoDock Vina: improving the speed and accuracy of docking with a new scoring function, efficient optimization, and multithreading. *J. Comput. Chem.* 31, 455–461.
- Wang, L., Li, C., Zhang, Y., Qiao, C., Ye, Y., 2013. Synthesis and biological evaluation of benzofuroxan derivatives as fungicides against phytopathogenic fungi. *J. Agric. Food Chem.* 61, 8632–8640.
- Wang, M.L., Rui, P., Liu, C.X., Du, Y., Qin, P.W., Qi, Z.Q., Ji, M.S., Li, X.H., Cui, Z.N., 2017. Design, synthesis and fungicidal activity of 2-substituted phenyl-2-oxo-, 2-hydroxy and 2-acyloxyethylsulfonamides. *Molecules* 22, 738.
- Wang, J.M., Wolf, R.M., Caldwell, J.W., Kollman, P.A., Case, D.A., 2004. Development and testing of a general amber force field. *J. Comput. Chem.* 25, 1157–1174.
- Wang, J.M., Wang, W., Kollman, P.A., Case, D.A., 2006. Automatic atom type and bond type perception in molecular mechanical calculations. *J. Mol. Graph. Model.* 25, 247–260.
- Wang, W., Zhang, S., Wang, J.H., Wu, F.R., Wang, T., Xu, G., 2021. Bioactivity-guided synthesis accelerates the discovery of 3-(iso)quinolinyl-4-chromenones as potent fungicide candidates. *J. Agric. Food Chem.* 69, 491–500.
- Wu, Z.B., Park, H.Y., Xie, D.W., Yang, J.X., Hou, S.T., Shahzad, N., Kim, C.K., 2021. Yang, S., Synthesis, Biological Evaluation, and 3D-QSAR Studies of N-(Substituted pyridine-4-yl)-1-(substituted phenyl)-5-trifluoromethyl-1H-pyrazole-4-carboxamide Derivatives as Potential Succinate Dehydrogenase Inhibitors. *J. Agric. Food Chem.* 69, 1214–1223.
- Yan, W., Wang, X., Li, K., Li, T.X., Wang, J.J., Yao, K.C., Cao, L.L., Zhao, S.S., Ye, Y.H., 2019. Design, synthesis, and antifungal activity of carboxamide derivatives possessing 1,2,3-triazole as potential succinate dehydrogenase inhibitors. *Pestic. Biochem. Physiol.* 156, 160–169.
- Yang, Z.H., Sun, Y., Liu, Q.S., Li, A.L., Wang, W.Y., Gu, W., 2021. Design, Synthesis, and Antifungal Activity of Novel Thiophene/Furan-1,3,4-Oxadiazole Carboxamides as Potent Succinate Dehydrogenase Inhibitors. *J. Agric. Food Chem.* 69, 13373–13385.
- Yang, D., Zhao, B., Fan, Z., Yu, B., Zhang, N., Li, Z., Zhu, Y., Zhou, J.H., Kalinina, T.A., Glukhareva, T.V., 2019. Synthesis and biological activity of novel succinate dehydrogenase inhibitor derivatives as potent fungicide candidates. *J. Agric. Food Chem.* 67, 13185–13194.
- Yao, T.T., Fang, S.W., Li, Z.S., Xiao, D.X., Cheng, J.L., Ying, H.Z., Du, Y.J., Zhao, J.H., Dong, X.W., 2017a. Discovery of novel succinate dehydrogenase inhibitors by the integration of in silico library design and pharmacophore mapping. *J. Agric. Food Chem.* 65, 3204–3211.
- Yao, T.T., Xiao, D.X., Li, Z.S., Cheng, J.L., Fang, S.W., Du, Y.J., Zhao, J.H., Dong, X.W., Zhu, G.N., 2017b. Design, synthesis, and fungicidal evaluation of novel pyrazole-furan and pyrazole-pyrrole carboxamide as succinate dehydrogenase inhibitors. *J. Agric. Food Chem.* 65, 5397–5403.
- Yoon, M., Cha, B., Kim, J., 2013. Recent trends in studies on botanical fungicides in agriculture. *Plant. Pathol.* 29, 1–9.
- Yu, B., Zhou, S., Cao, L.X., Hao, Z.S., Yang, D.Y., Guo, X.F., Zhang, N.L., Bakulev, V.A., Fan, Z.J., 2020. Design, Synthesis, and Evaluation of the Antifungal Activity of Novel Pyrazole-Thiazole Carboxamides as Succinate Dehydrogenase Inhibitors. *J. Agric. Food Chem.* 68, 7093–7102.
- Zhang, L., Li, W., Xiao, T., Song, Z., Csuk, R., Li, S.K., 2018b. Design and discovery of novel chiral antifungal amides with 2-(2-oxazolonyl)aniline as a promising pharmacophore. *J. Agric. Food Chem.* 66, 8957–8965.
- Zhang, A., Zhou, J., Tao, K., Hou, T., Jin, H., 2018a. Design, synthesis and antifungal evaluation of novel pyrazole carboxamides with diarylamines scaffold as potent succinate dehydrogenase inhibitors. *Bioorg. Med. Chem. Lett.* 28, 3042–3045.
- Zhang, A., Yue, Y., Yang, J., Shi, J., Tao, K., Jin, H., Hou, T.P., 2019. Design, synthesis, and antifungal activities of novel aromatic carboxamides containing a diphenylamine scaffold. *J. Agric. Food Chem.* 67, 5008–5016.